Electron-Beam Based Neutron Sources

BE Department Seminars
8th of November, 2024

Javier Olivares Herrador [1,2], Lawrence M. Wroe[1], Andrea Latina[1], Walter Wuensch[1], Steinar Stapnes[1], Nuria Fuster-Martinez[2], Benito Gimeno[2], Daniel Esperante[2].

[1] CERN, Meyrin, 1217, Switzerland.
[2] Instituto de Física Corpuscular (IFIC), CSIC-University of Valencia. Calle Catedrático José Beltrán Martínez, 2, 46980 Paterna (Valencia), Spain

Is an electron linac a suitable driver for neutron production?

To answer this question, I will discuss:

I. The **necessity** for neutron sources & **mechanisms** of neutron production

II. Unmoderated neutron **spectrum characterization**

III. Challenges in the use of **high-intensity** electron linacs

  I. Comparison with the **state-of-the-art**

IV. Neutron moderation and **brightness/brilliance** discussion

V. **VULCAN** project

VI. Conclusions

I. Necessity for neutron sources

- **Uprising demand**: Wide variety of research areas make use of neutrons
  - Not only research: Industrial and medical applications! [1, 2]

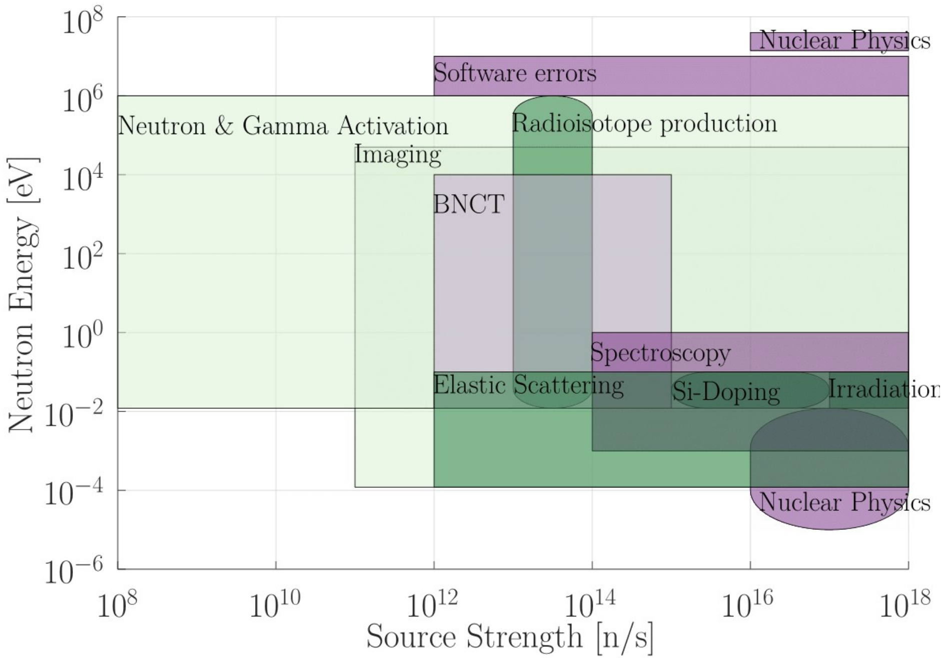

I. Neutron production with accelerators

- Neutron sources migrating from nuclear reactors to **accelerator-based facilities** [3]
- **Hadron**-based machines. **Direct** processes:
  - Spallation
  - Controlled nuclear reaction:

$$p + {}^{7}\mathrm{Li} \rightarrow n + {}^{7}\mathrm{Be}$$

- **Electron**-based machines. Indirect process:
  - Bremmstrahlung + Photonuclear reaction

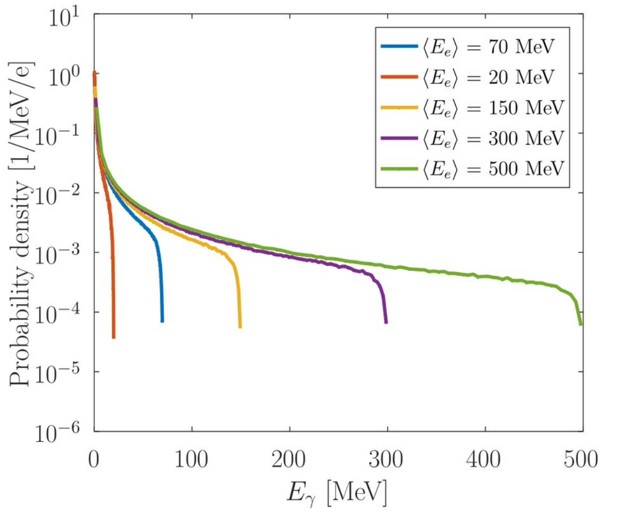

Bremmstrahlung spectrum for different electron beams against tungsten.

I. Neutron production with accelerators

- Neutron sources migrating from nuclear reactors to **accelerator-based facilities** [3]
- **Hadron**-based machines. **Direct** processes:
  - Spallation
  - Controlled nuclear reaction:

$$p + {}^{7}\mathrm{Li} \rightarrow n + {}^{7}\mathrm{Be}$$

- **Electron**-based machines. Indirect process:
  - Bremmstrahlung + Photonuclear reaction

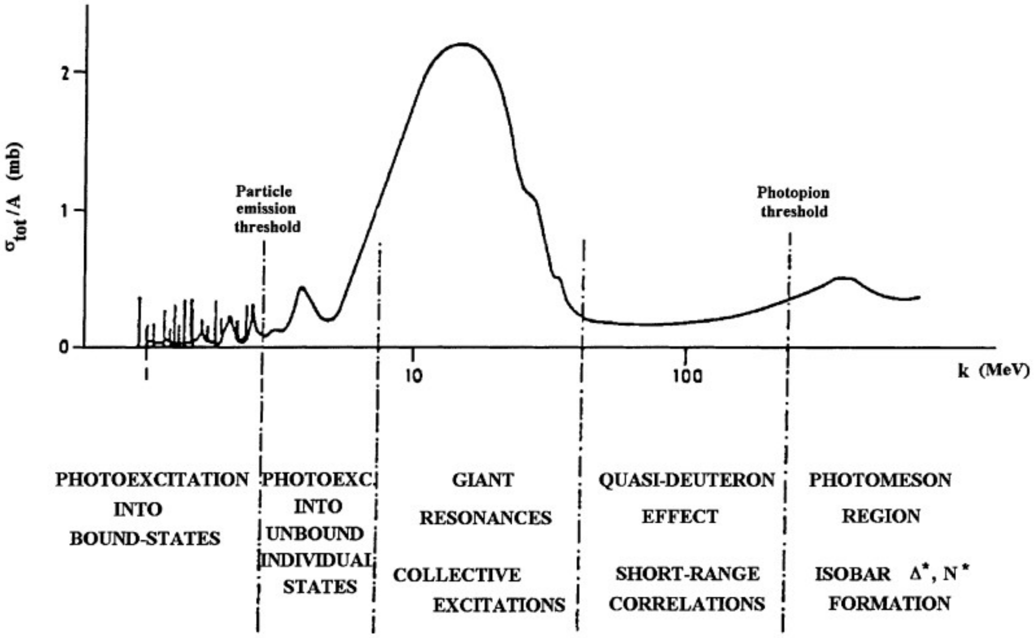

Photonuclear cross section W(g,n).

II. Neutron production with electrons

- Single tungsten target where **both** processes occur
- G4beamlines simulations [4]
  - Optimal dimensions: r = 40mm; L = 80 mm

$$Y_n(E_e) \equiv \frac{N_n(E_e)}{N_e}$$

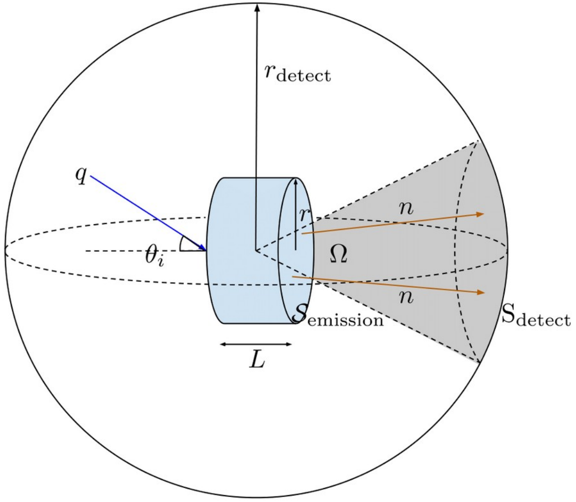

Neutron production setup

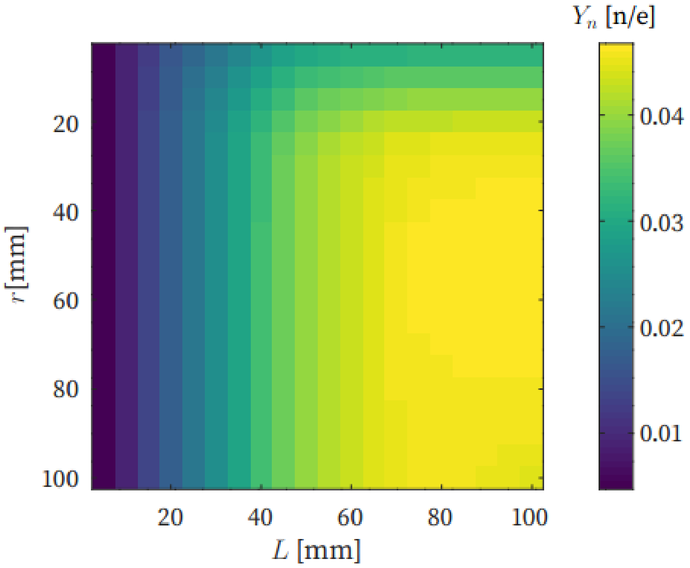

Dimensions scan for maximum yield for <Ee> = 500 MeV

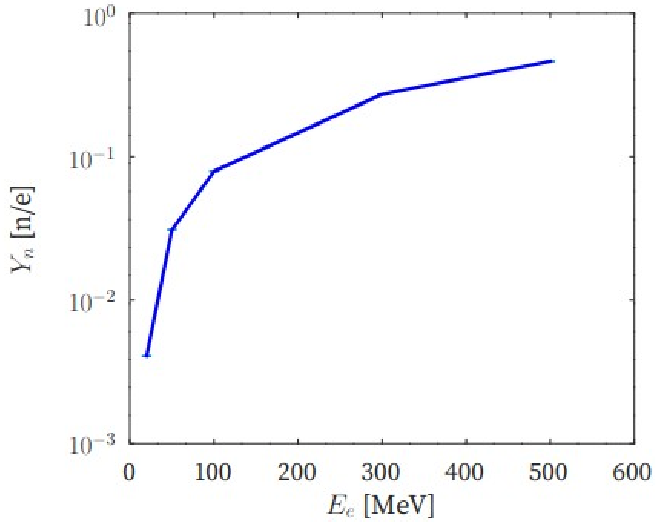

Optimal yields for different energies

II. Unmoderated neutron spectrum

- For the optimized W target, we note:
  - Backward emission > Forward emission
  - Plateau of ~40 deg around max emission (130deg)

$$f_\Omega(\varphi, \theta_d; E_e) \equiv \frac{d^2 Y_n}{d\Omega}(\varphi, \theta_d)$$

$$f_\theta(\theta_d; E_e) \equiv \frac{1}{2\pi} \int_0^{2\pi} f_\Omega(\theta_d, \varphi) d\varphi$$

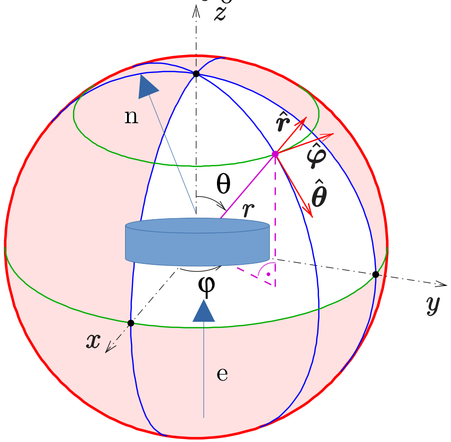

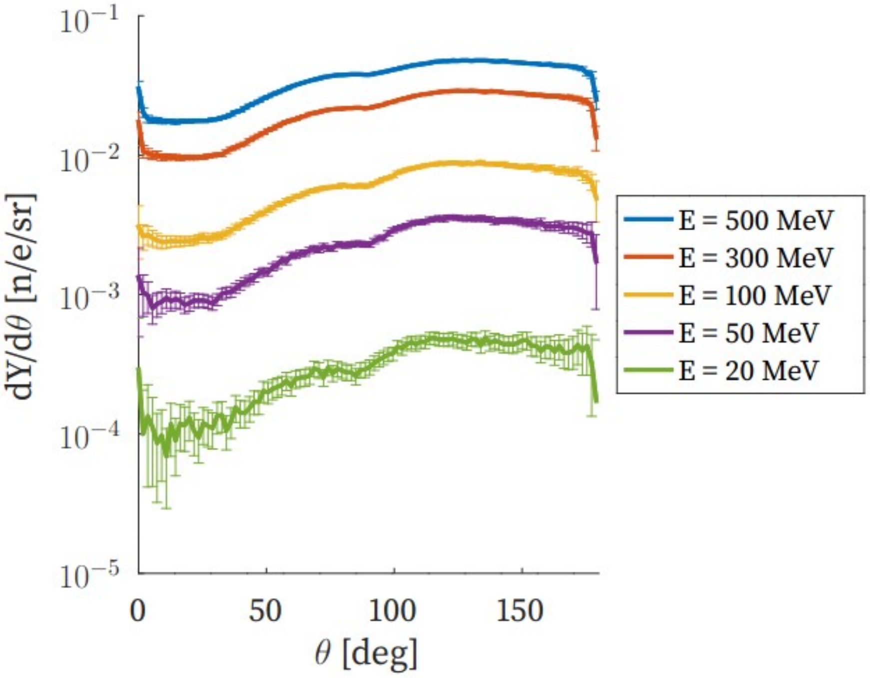

Neutron detection dependency with incidence angle and <Ee> = 500 MeV and θ_i = 0 deg.

II. Unmoderated neutron spectrum

- For the optimized W target, we note:
  - Backward emission > Forward emission
  - Plateau of ~40 deg around max emission (130deg)
  - Maxwellian neutron emission with ‹E_n› ~ 1 MeV

$$f_{\theta,E_n}(\theta_d, E_n; E_e) \equiv \frac{\mathrm{d}f_\theta}{\mathrm{d}E_n}$$

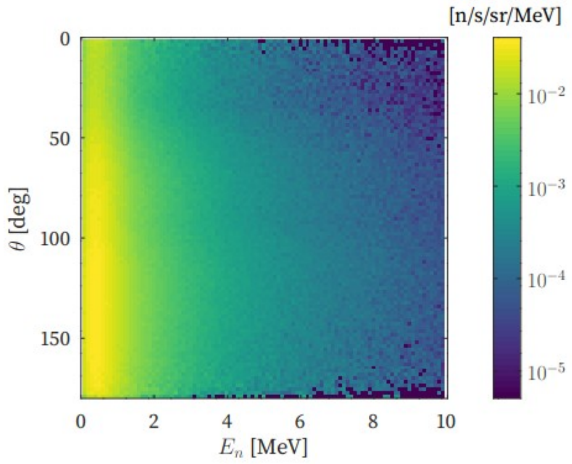

Energy distribution for different detecting angles.
‹E_e› = 500 MeV

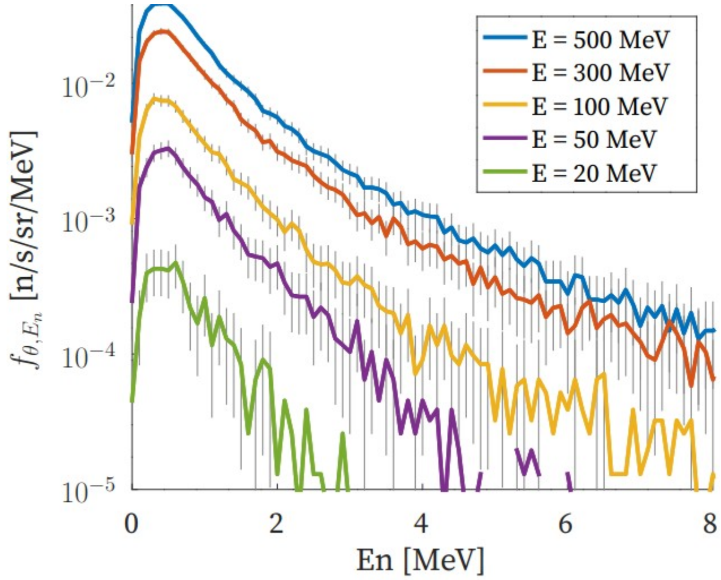

Energy distribution for different detecting angles.
θi = 0 deg; θd = 130 deg. For different energies

III. High intensity e-linac proposals

- Targeted figure of merit: **Source strength**

$$I_n \equiv I_{e,\mathrm{av}} Y_n$$

- Two normal-conducting high-intensity linacs are considered
  - **HPCI – linac**: S-band Photoinjector + X-band TW structures [5]
  - **CTF3 drive-beam linac**: S-band Thermoionic gun + S-band TW structures [6]

Magnitude	**Units**	**HPCI-linac**	**CTF3 drive beam linac**
f	GHz	12.00	3.00
Q_{bunch}	nC	0.285	2.33
N_{bunches}		1000	2100
$f_{\text{RF-cycle}}$	Hz	100	100
$I_{e,\mathrm{av}}$	μA	28.50	489.3

High-intensity compact linac specifications [5, 6]

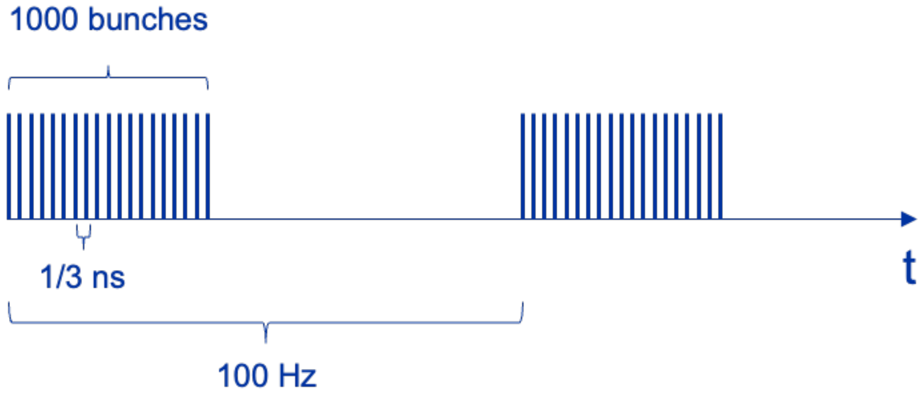

Train schematics for the HPCI linac

III. Full Beam Loading Operation

- **Beam Loading**: Gradient reduction due to beam-cavity interaction
  - The beam excites the fundamental mode in the decelerating phase

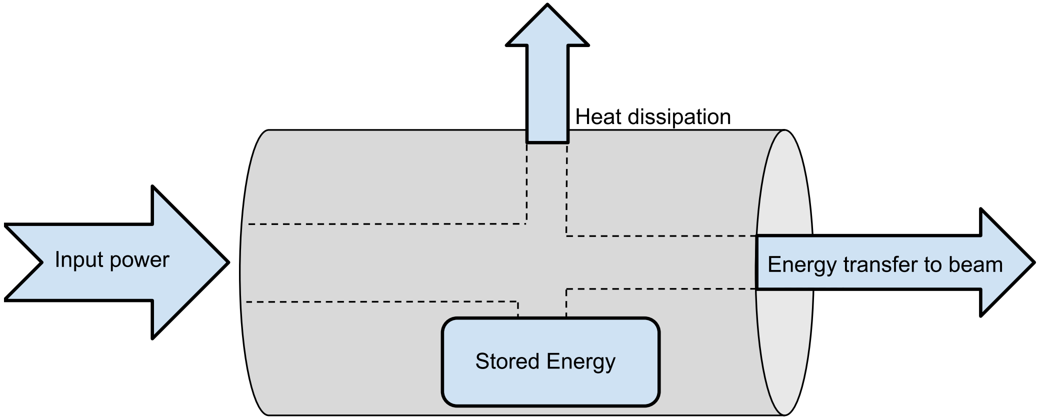

- Implemented in **RF-Track**: In-house particle tracking code
  - Allows tracking of macroparticle bunches in complex 3D fieldmaps considering collective effects
  - Interface with Python and Octave

III. Full Beam Loading Operation

- **Beam Loading**: Gradient reduction due to beam-cavity interaction
- **Full Beam Loading**: High intensity so that **all energy is substracted** from the structure

f_b [GHz]	q_{bunch} [pC]	min. N_{bunches}
12.00	150.6	657
6.00	301.2	329
4.00	451.8	219
3.00	602.4	165
2.00	903.6	110
1.50	1204.8	83

Full BL configurations (refer to steady state)

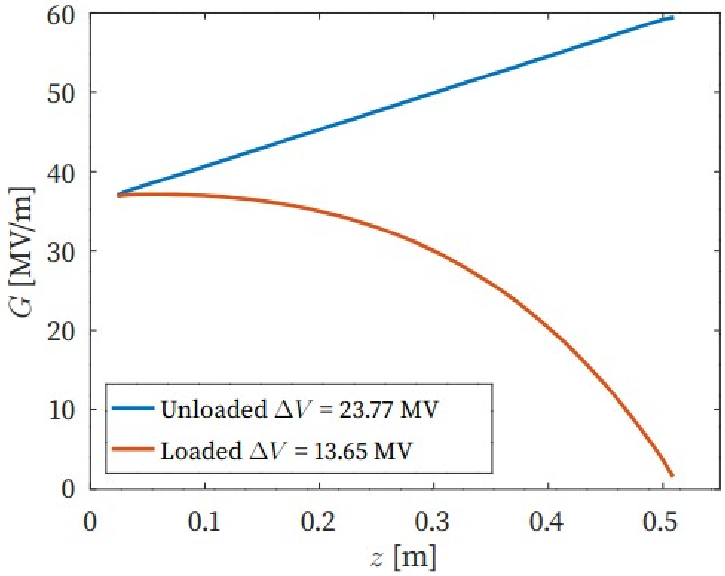

Accelerating gradient of an HPCI X-band linac in full BL operation

III. Full Beam Loading Operation

- **Beam Loading**: Gradient reduction due to beam-cavity interaction
- **Full Beam Loading**: High intensity so that **all energy is substracted** from the structure

f_b [GHz]	q_{bunch} [pC]	min. N_{bunches}
12.00	150.6	657
6.00	301.2	329
4.00	451.8	219
3.00	602.4	165
2.00	903.6	110
1.50	1204.8	83

I use 1000 bunches

Full BL configurations (refer to steady state)

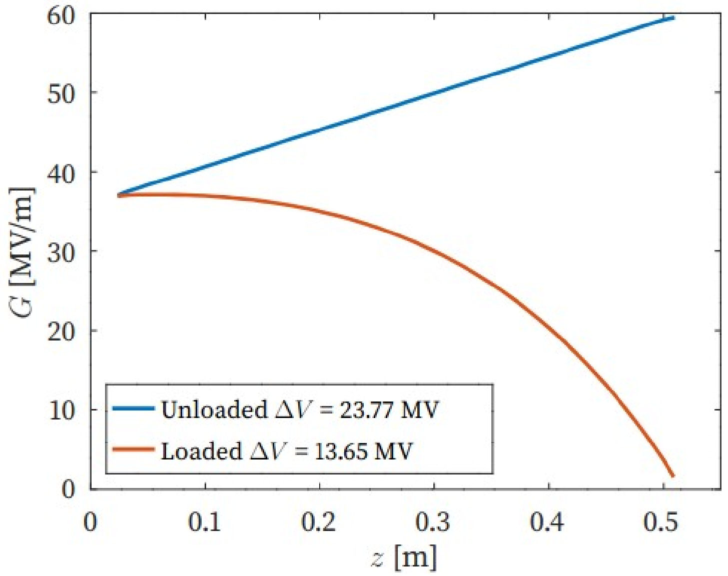

Accelerating gradient of an HPCI X-band linac in full BL operation

Challenges: Beam dynamics, heat deposition

III. Full Beam Loading Operation

- **Beam Loading**: Gradient reduction due to beam-cavity interaction
- **Full Beam Loading**: High intensity so that **all energy is substracted** from the structure
- Despite BL being inherent, it **maximizes the RF-to-beam efficiency.**

$$\eta = \frac{\Delta P_{\mathrm{beam}}(t)}{P_{\mathrm{in}}(t)} = \frac{I(t)}{P_{\mathrm{in}}(t)} \int_0^L G(z,t)\mathrm{d}z = 0.927$$

$$\eta_{\mathrm{av}} = \frac{\int_0^{T_{\mathrm{pulse}}} \Delta P_{\mathrm{beam}}(t)\ \mathrm{d}t}{\int_0^{T_{\mathrm{pulse}}} P_{\mathrm{in}}(t)\ \mathrm{d}t} = 0.896$$

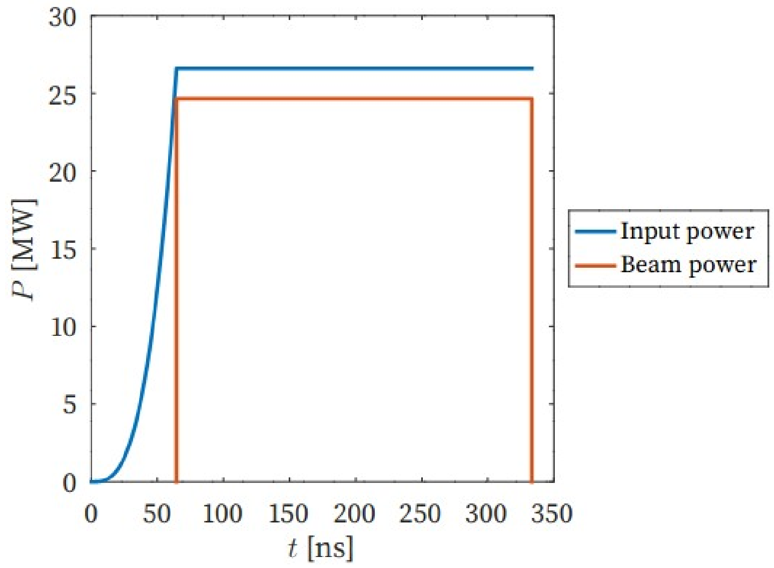

RF power and beam energy gain power

III. Heat Deposition

- Non-uniform energy deposition → Large temperature increase → Non-elastic mechanical stresses
- Depends on beam intensity and beam size ($\sigma_x = \sigma_y = 1.3$ mm)

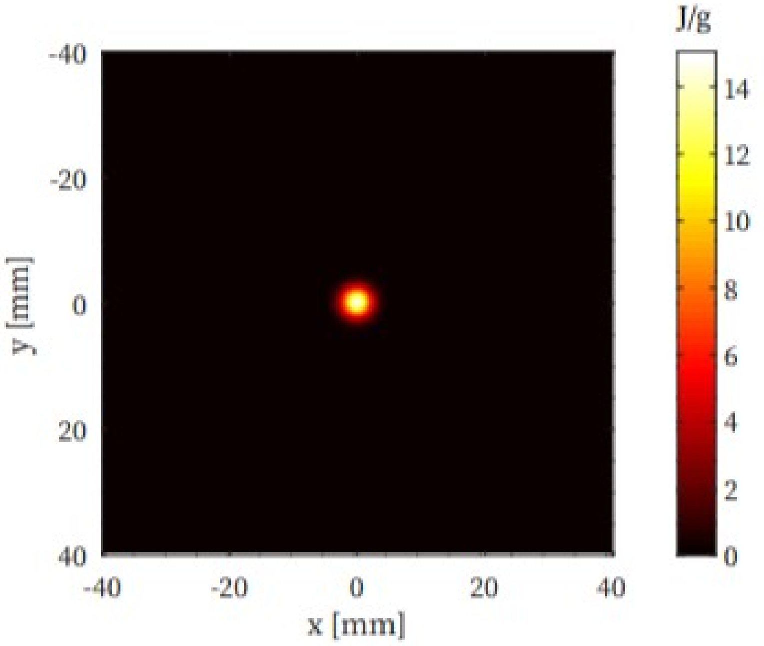

Heat deposition profile at z= 0 mm.

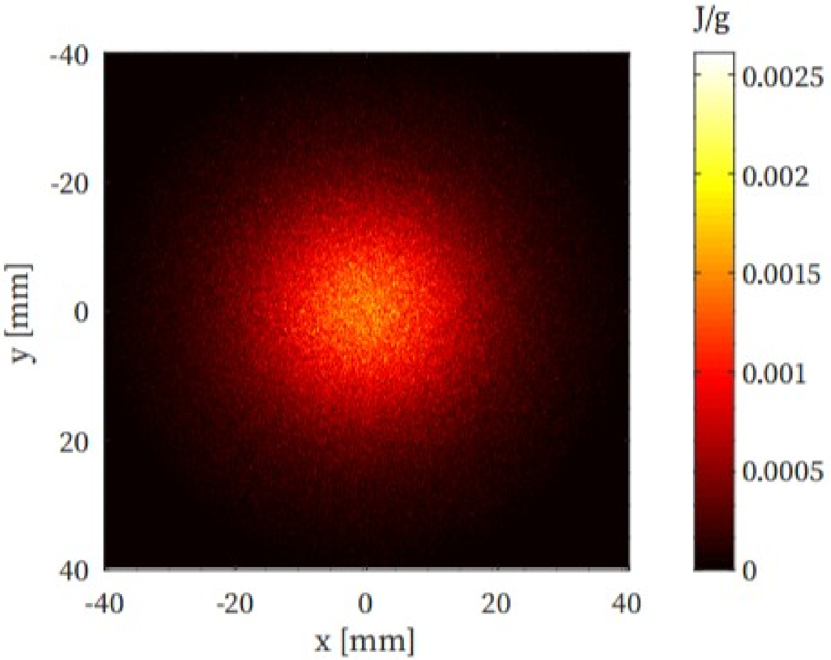

Heat deposition profile at z = 80 mm.

III. Heat Deposition

- Non-uniform energy deposition → Large temperature increase → Non-elastic mechanical stresses
- Depends on beam intensity and beam size ($\sigma_x = \sigma_y = 1.3$ mm)
- Pure tungsten: Limit of 35 J/g

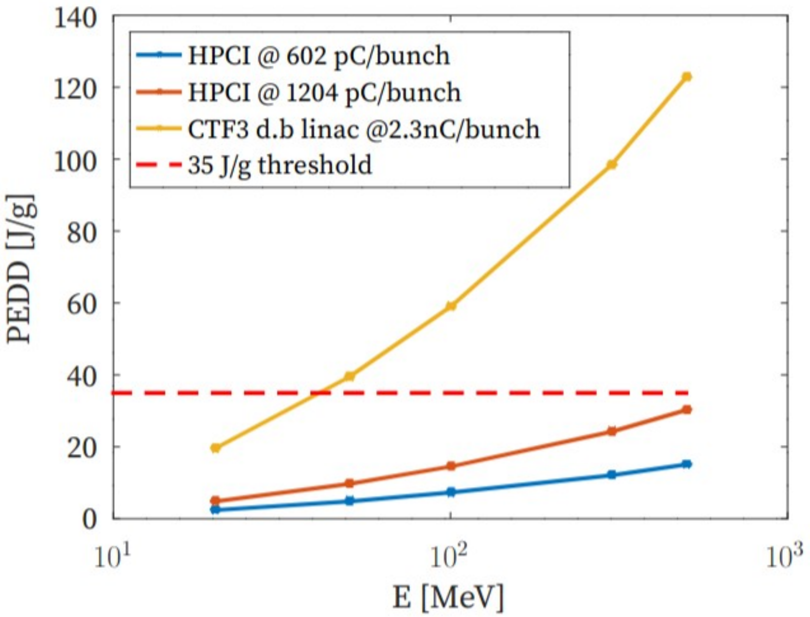

PEDD values for the different e-linac proposals with $\sigma_x = \sigma_y = 1.3$ mm

III. Heat Deposition

- Non-uniform energy deposition → Large temperature increase → Non-elastic mechanical stresses
- Depends on beam intensity and beam size ($\sigma_x = \sigma_y = 1.3$ mm)
- Pure tungsten: Limit of 35 J/g

For CTF3, PEDD @ 500 MeV exceeds the 35 J/g limit by a factor 4.
Transverse beam size can be aumented a factor 2

→ Necessity to carry out **beam dynamics** simulations

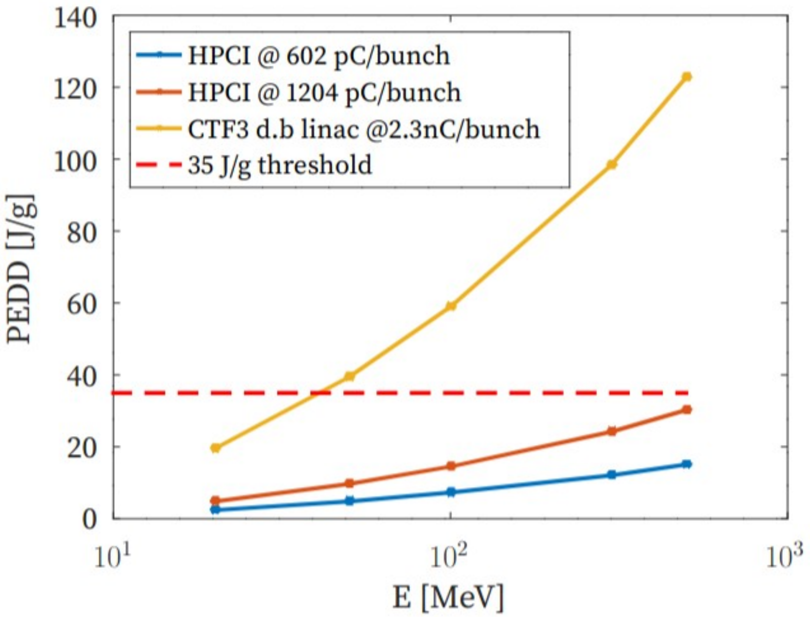

PEDD values for the different e-linac proposals with $\sigma_x = \sigma_y = 1.3$ mm

III. State-of-the-art comparison

$$P_{\text{beam}} = I \cdot E/e$$

[7]

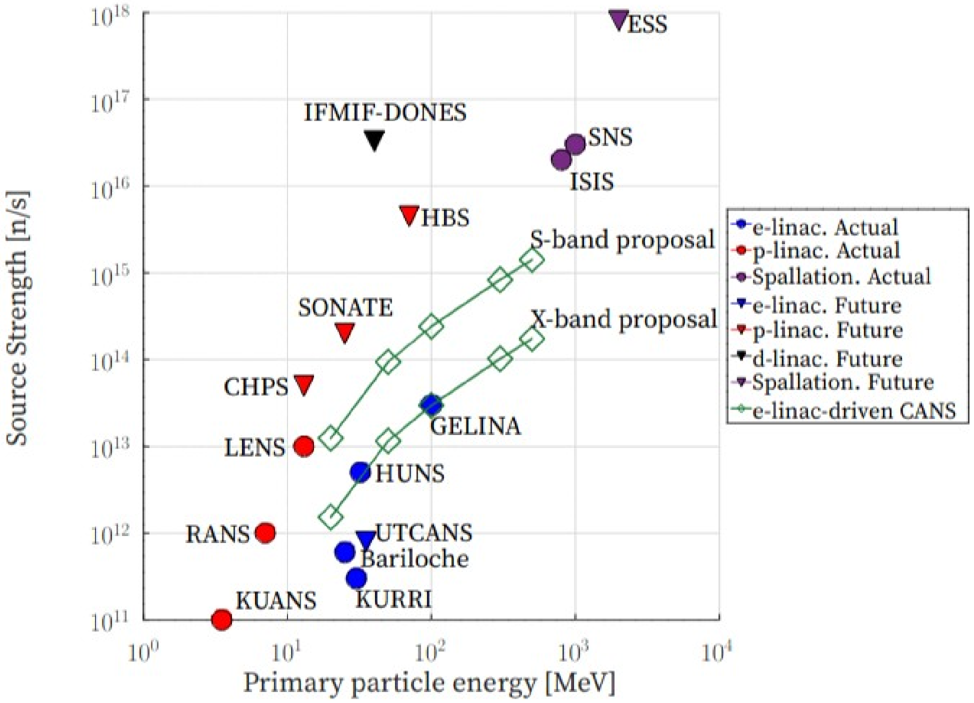

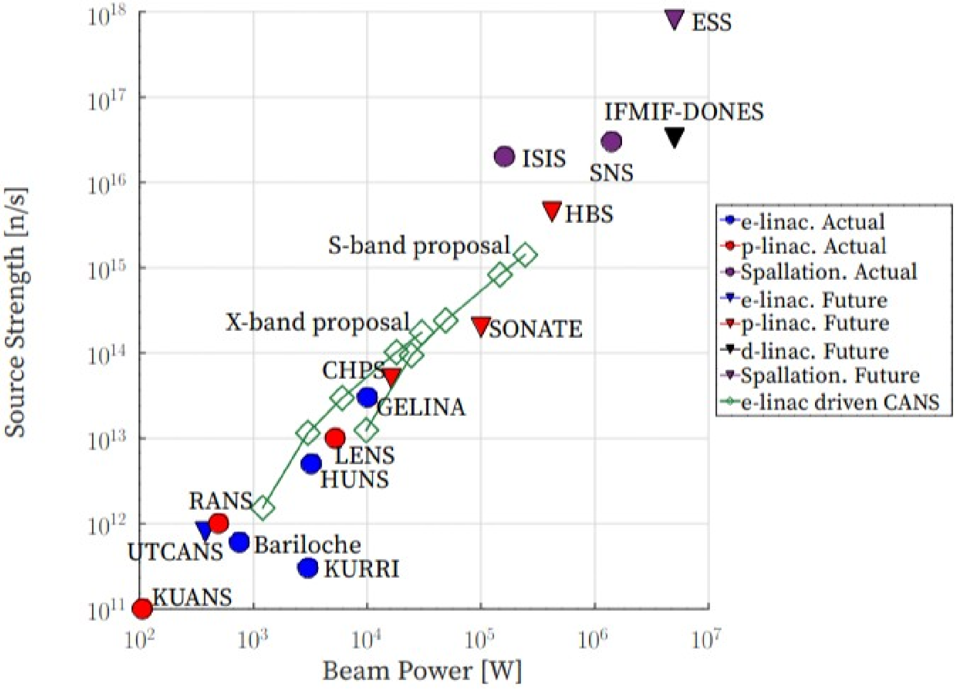

III. State-of-the-art comparison

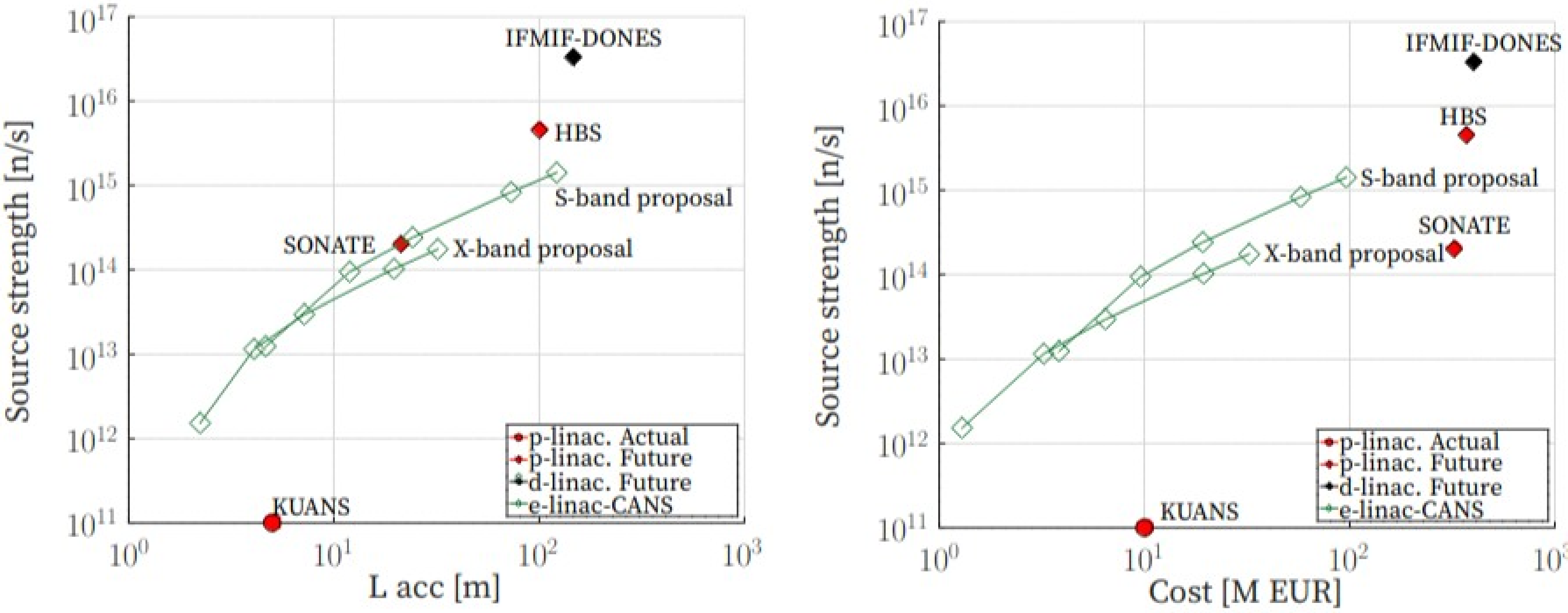

III. Efficiency comparison

Magnitude	Unit	HPCI - 602pC/bunch	CTF3 S-band
Beam power gain	MW	24.6	26.6
Pulse length	μs	0.333	1.56
Energy required in 2 structures		16.86	82.93
f_{RF}	Hz	100	100
Loaded gradient	MV/m	27.0	6.5
Pairs of structures		16	28
Total length	m	24.0	112.3
η, total wall-beam efficiency		0.27	0.24
Energy consumed by a train	J	986.2	9587
Yield	n/s	$1.74 \cdot 10^{14}$	$1.42 \cdot 10^{15}$
Cost of a neutron	J/n	$5.65 \cdot 10^{-10}$	$6.76 \cdot 10^{-10}$

Efficiency comparison for both electron linac proposals at 500 MeV.

HBS
$2.7 \cdot 10^{-9}$ J/n

IV. Thermal and cold neutron moderation

- Material science: **Diffractrometry** and **imaging** experiments
  - Require moderated neutrons – rich **H compounds**
- Targeted figure of merit: **Average brightness**

$$f_\lambda(\theta, \lambda; E_e) \equiv \frac{\mathrm{d}^3 I_{\mathrm{n,\ av}}}{\mathrm{d}S_{\mathrm{emission}}\mathrm{d}\Omega\mathrm{d}\lambda}$$

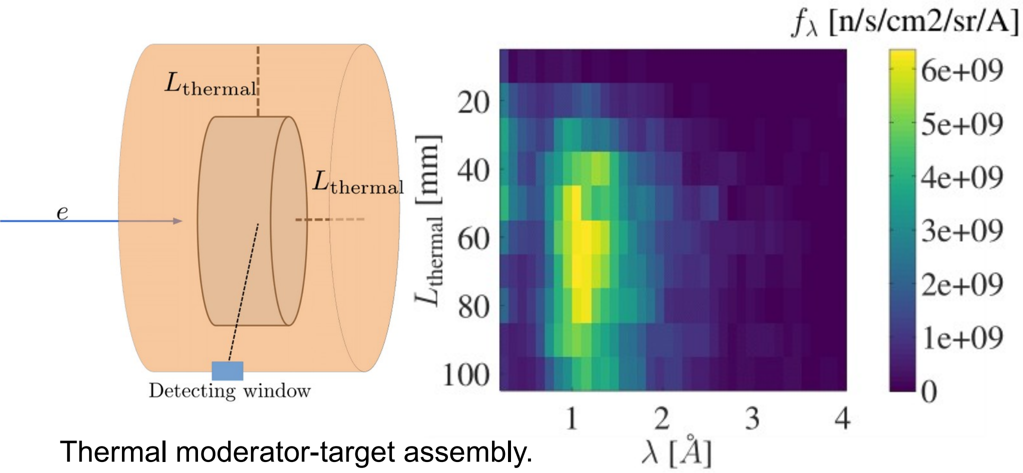

Thermal moderator-target assembly.
CH_4 layer

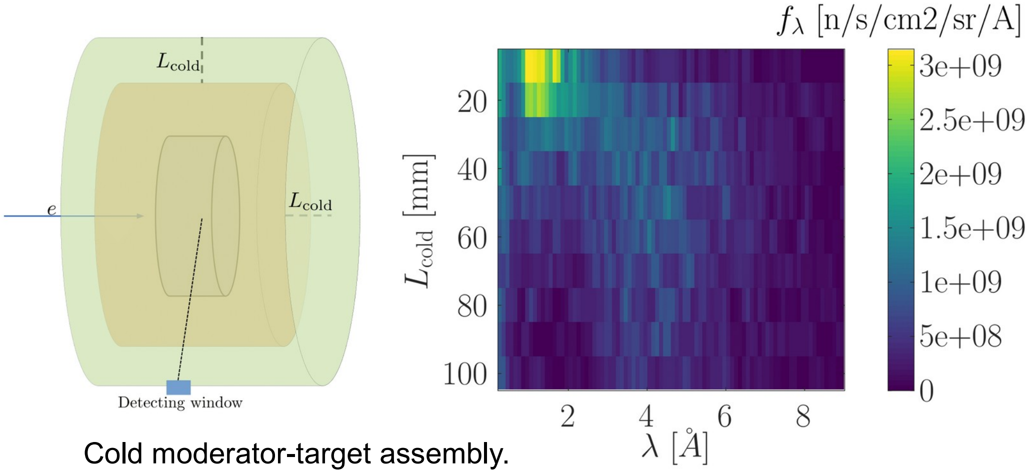

Cold moderator-target assembly.
Liquid H_2 (20K) layer

- **Optimal dimensions:** L_{thermal} = 60 mm; L_{cold} = 25 mm.

IV. Thermal and cold neutron detection

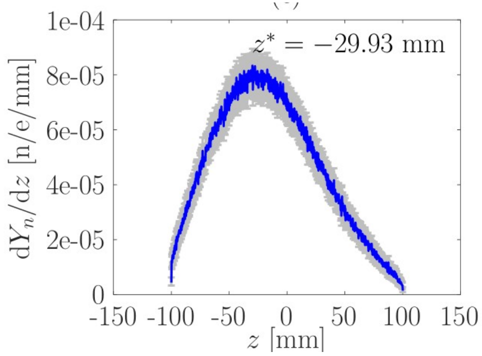

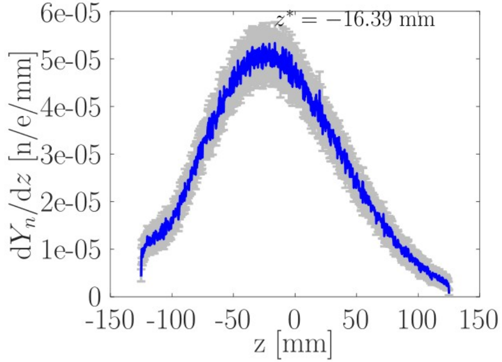

Backward/Lateral maximum emission

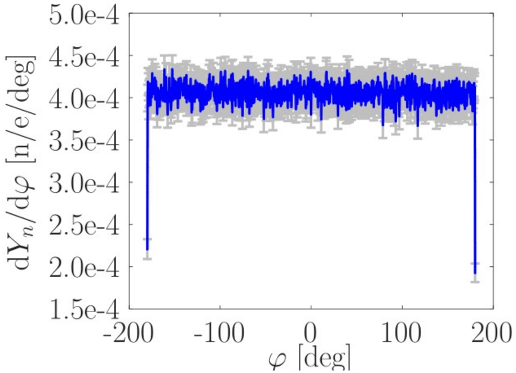

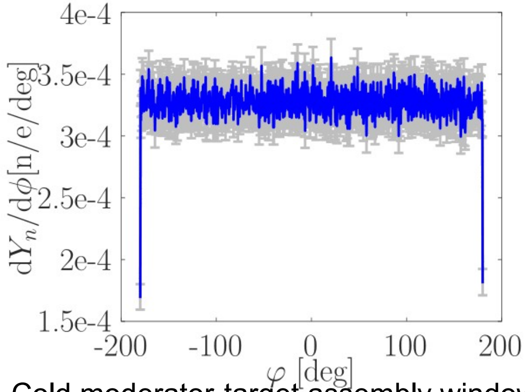

Azimutal isotropy

Thermal moderator-target assembly window location (up) and azimutal dependency of the yield (down)

Cold moderator-target assembly window location (up) and azimutal dependency of the yield (down)

IV. Average Brightness

- Proportional to electron intensity (CTF3 > HPCI)

CTF3 d.b - thermal

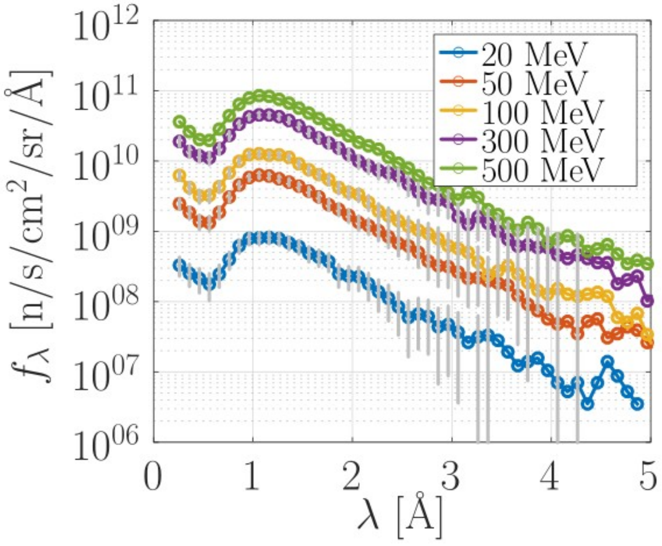

Thermal moderator-target average brightness for different electron energies for CTF3 drive beam linac.

HPCI - thermal

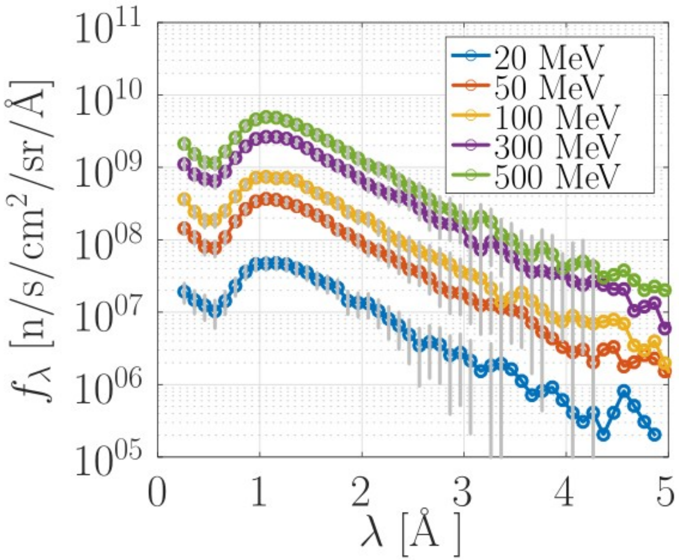

Thermal moderator-target average brightness for different electron energies for HPCI linac.

IV. Average Brightness

- Proportional to electron intensity (CTF3 > HPCI)

CTF3 d.b - Cold

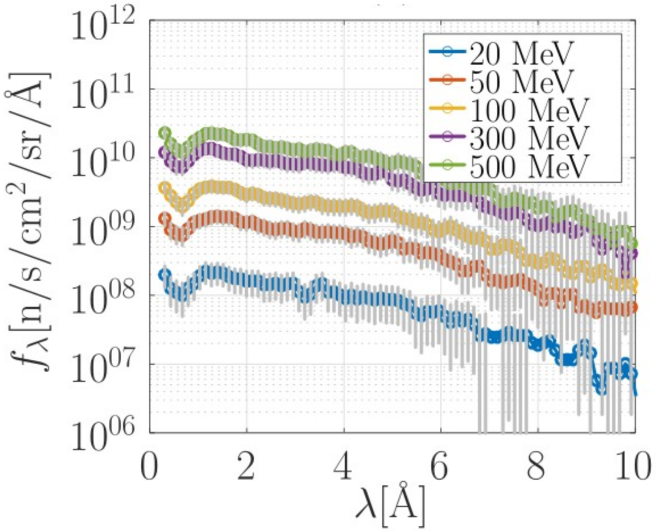

Cold moderator-target average brightness for different electron energies for CTF3 drive beam linac.

HPCI - Cold

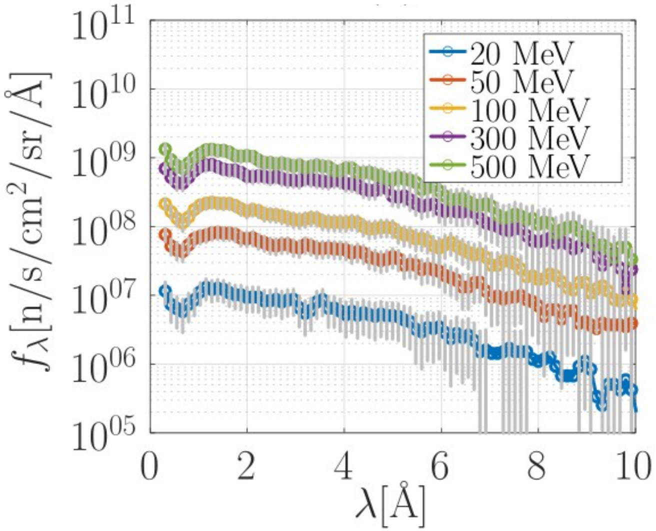

Cold moderator-target average brightness for different electron energies for HPCI linac.

IV. Peak brightness

- Time-resolution of the brightness spectrum
  - Convolves electron pulse with neutron response

$$f_{\lambda,\ \mathrm{peak}} \equiv \max_{t>0}\left(\frac{\mathrm{d}q_e}{\mathrm{d}t} \otimes g_{\lambda,t}\right) \qquad g_{\lambda,t} \equiv \frac{{}^{4}Y_n}{\mathrm{d}S_{\mathrm{emission}}\mathrm{d}\Omega\mathrm{d}\lambda\mathrm{d}t}$$

- Cold and thermal **neutron** responses extend **several μs.** GHz **electron** pulses extend **100s ns**

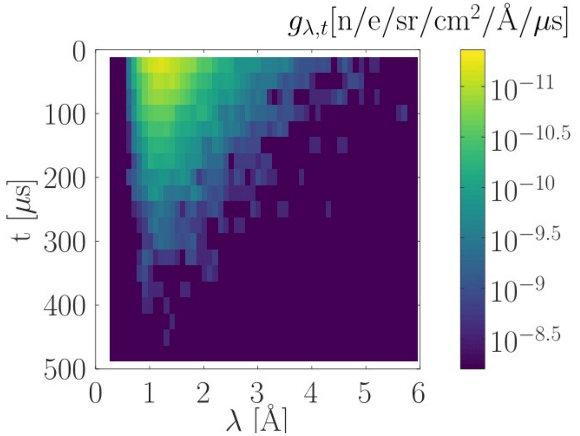

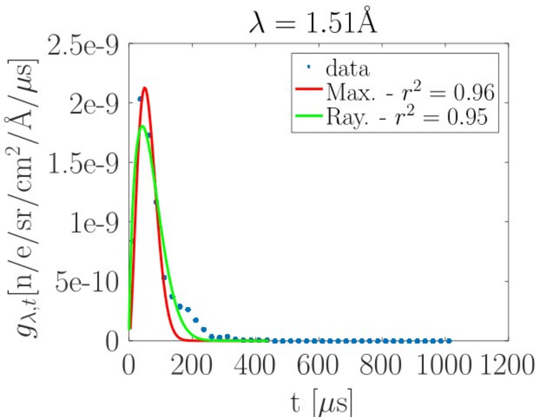

$\otimes$

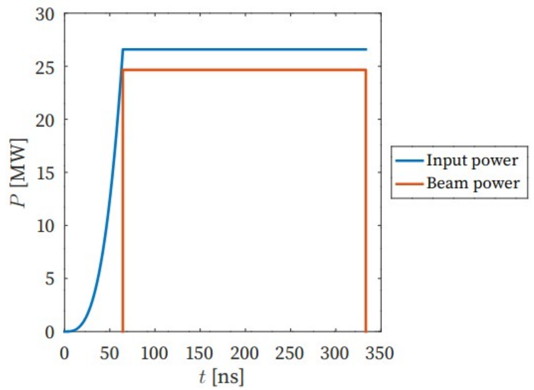

IV. Peak brightness

- For the case of electron trains (few ns), the peak brightness is just the normalization of g_λ to the total train charge.

CTF3 d.b - thermal

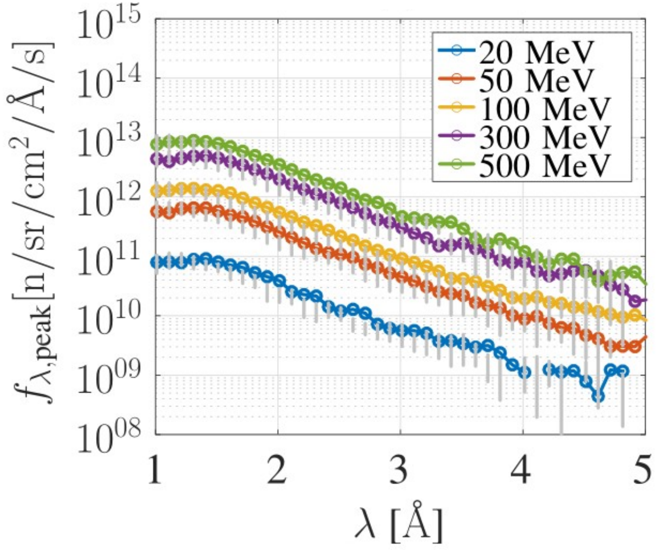

Thermal moderator-target peak brightness for different electron energies for CTF3 drive beam linac.

HPCI - thermal

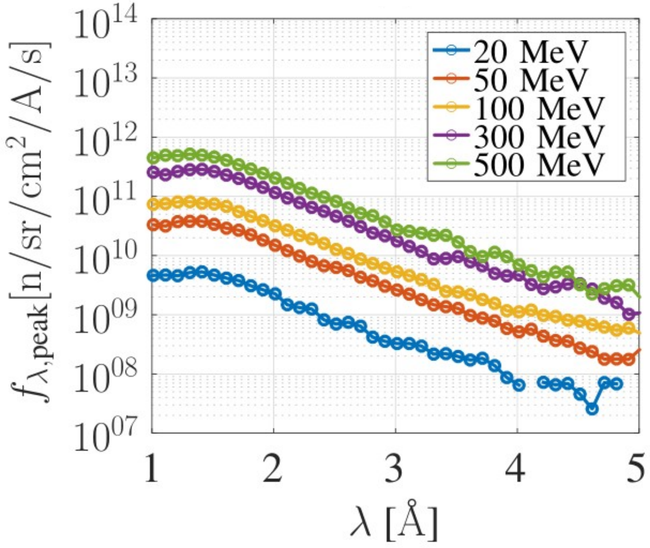

Thermal moderator-target peak brightness for different electron energies for HPCI linac.

IV. Peak brightness

- For the case of electron trains (few ns), the peak brightness is just the normalization of g_λ to the total train charge.

CTF3 d.b - Cold

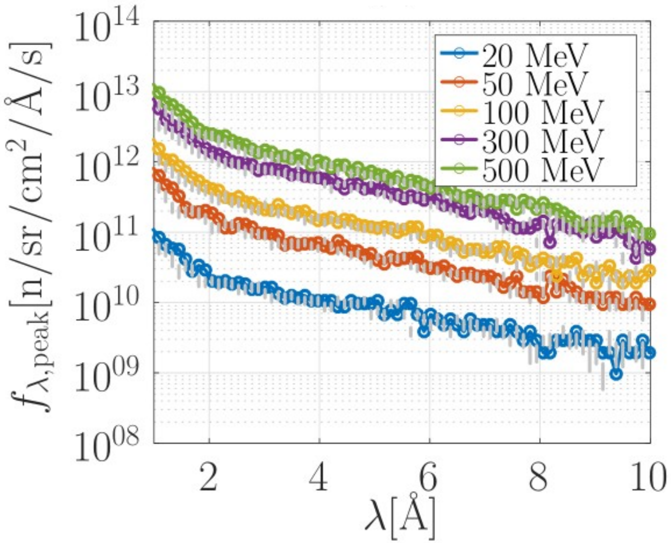

Cold moderator-target peak brightness for different electron energies for CTF3 drive beam linac.

HPCI - Cold

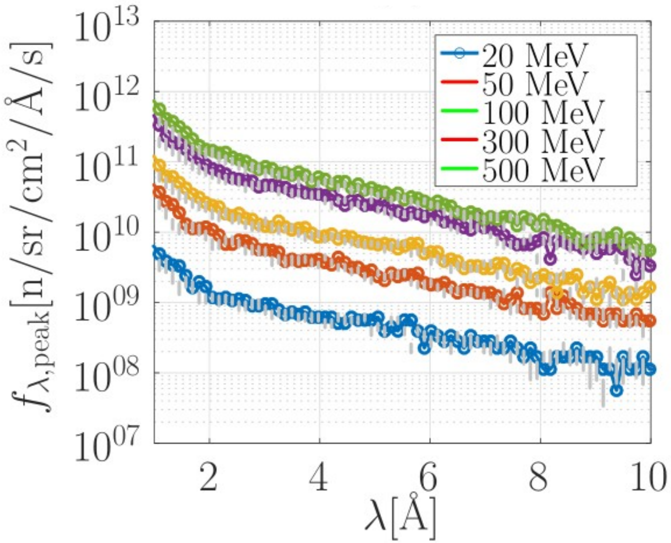

Cold moderator-target peak brightness for different electron energies for HPCI linac.

IV. Brightness State-of-the-art comparison

- [7] [8] [9]

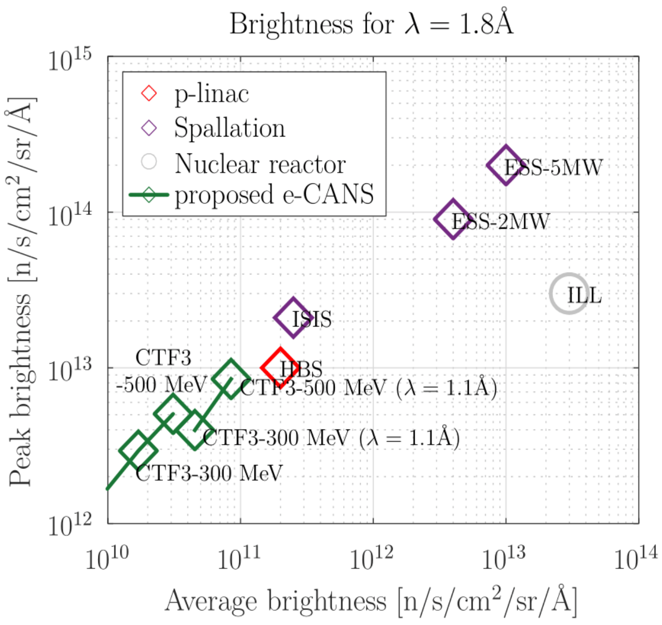

Thermal neutron brightness state-of-the-art.

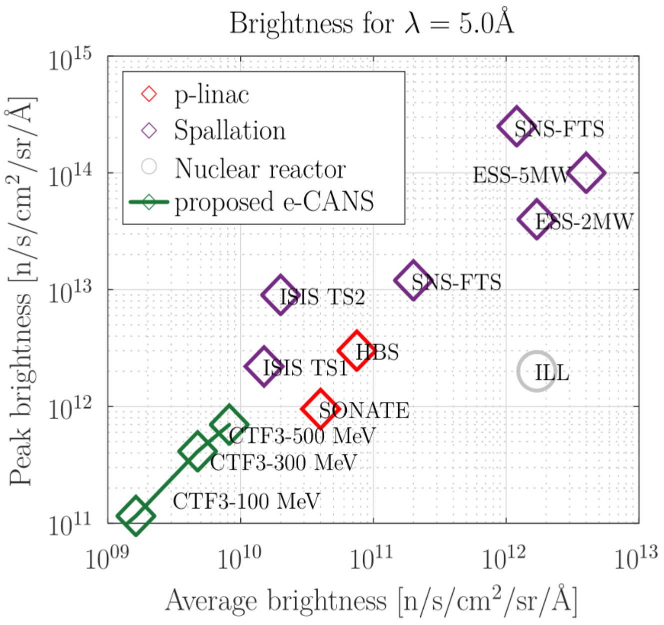

Cold neutron brightness state-of-the-art.

V. VULCAN

- **Commercial off-the-shelf** CANS (compact accelerator-based neutron source) **[10]**
- **VULCAN** = **V**ersatile **UL**tra **C**ompact **A**ccelerator-based **N**eutron source
- Collaboration between DAES SA and CERN → Industrial implementation

- Targeted applications:
  - In-situ **analysis** of **battery** and fuel cell **electrodes**
  - **Measurements** of internal **stresses** of **metallic** and **ceramic** components

Courtesy of L.M. Wroe

V. VULCAN

Parameter	Unit	Value
Energy	MeV	35
Energy spread	MeV	<5
Transverse size	mm	< 5
Transverse Jitter	mm	< 2
Train length	μs	<1
Train frequency	Hz	100-200

Electron beam requirements.

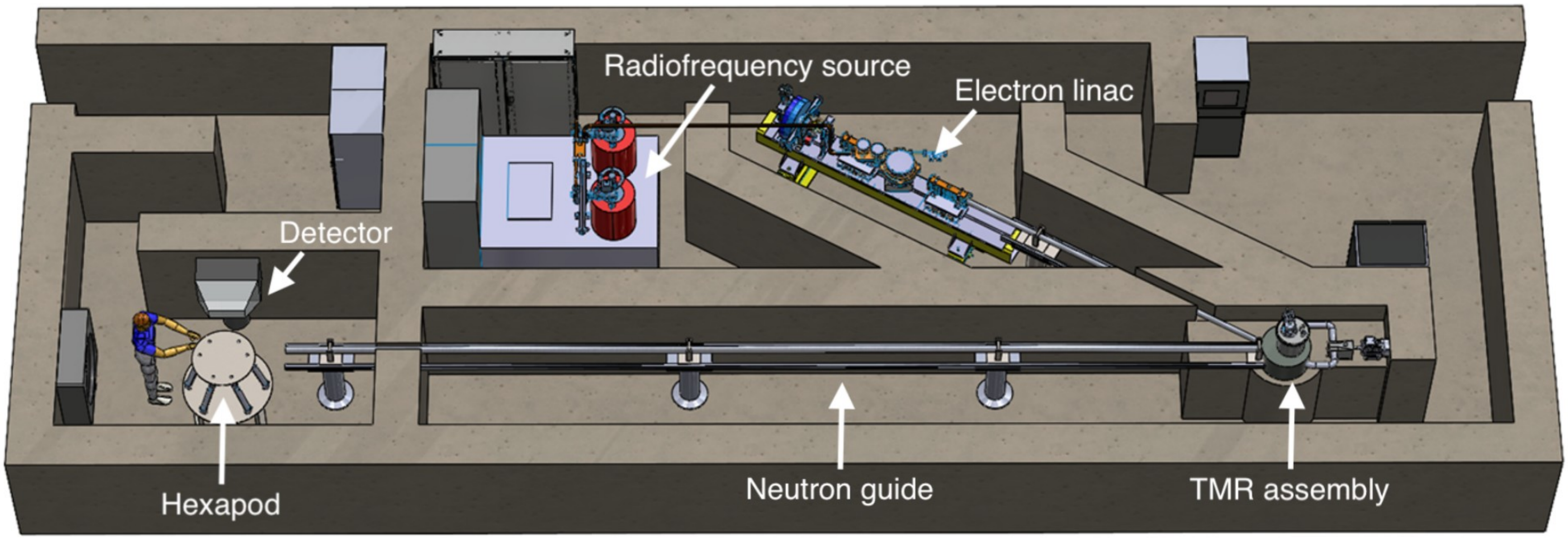

V. VULCAN

REQUIREMENTS

- Beam power: > 1 kW
  - Average beam current > 29 μA
- Peak beam Current > 290 mA
- Length: < 10 m
- Cost: < 5 M€

ACCELERATOR DESIGN CHOICES

- **Thermoionic** gun
  - High average intensities
- High gradient RF cavities **(3-12 GHz)**
  - TW: Compatible with pulse compressor
- RF power source: **klystron**
  - Peak power in 5-50 MW

Conclusions

- Neutrons are produced from electron beams by **Bremsstrahlung** + **Photonuclear excitation**
- Neutron production is a trade off between beam power, cost and length. Electron-linac-based neutron sources serve as **affordable & efficient** and middle-flux options
  - Eg: VULCAN – **compact**, suited for **industrial** purposes
- Electron linacs are suitable for **multi-purpose facilities** since the unmoderated energy spectrum does not vary strongly with the initial electron energy
  - Dfferent intensities can be achieved while keeping the same moderating scheme can be adopted for different values of ⟨Ee⟩.
- High-energy and high-intensity electron linacs (like CTF3 drive beam linac at 300, 500 MeV) can provide **bright neutron beams comparable** to proton-linac-based and spallation sources.

Further work

- Further beam dynamics simulations with RF-Track:
  - Focusing
  - Impact of BL and wakefields
- Specific target-moderator design to meet the requirements of a particular application
  - Further engineering aspects to be considered
- VULCAN: Beam dynamics and EM simulations ongoing
  - CDR in writing phase.

References

1) Y. Kiyanagi, “Neutron applications developing at compact accelerator-driven neutron sources,” *AAPPS Bulletin*, vol. 31, pp. 1–19, 2021.

2) *Compact Accelerator Based Neutron Sources*, ser. TECDOC Series. Vienna: INTERNATIONAL ATOMIC ENERGY AGENCY, 2021, no. 1981. [Online]. Available: https://www.iaea.org/publications/14948/compact-accelerator-based-neutron-sources

3) J. M. Carpenter, “The development of compact neutron sources,” *Nature Reviews Physics*, vol. 1, no. 3, pp. 177–179, 2019.

4) T. Roberts, “G4beamline user’s guide,” *Muons, Inc*, pp. 3468–3470, 2013.

5) A. Latina, V. Musat, R. Corsini, L. A. Dyks, E. Granados, A. Grudiev, S. Stapnes, P. Wang, W. Wuensch, E. Cormier, and G. Santarelli, “A compact inverse compton scattering source based on x-band technology and cavity-enhanced high average power ultrafast lasers,” in 67th *ICFA Adv. Beam Dyn. Workshop Future Light Sources Conference Proceedings*, 2023, pp. 257–260

6) G. Geschonke and A. Ghigo, “Ctf3 design report,” Tech. Rep., 2002.

References

7) J. Olivares Herrador, L.Wroe, A. Latina, et al. “Neutron production using compat linear electron accelerators”. JACoW **IPAC2024** (2024), MOPR93 doi:10.18429/JACoW-IPAC2024-MOPR93

8) T. Brückel, T. Gutberlet, J. Baggemann, S. Böhm, P. Doege, J. Fenske, M. Feygenson, A. Glavic, O. Holderer, S. Jaksch et al., *Conceptual Design Report-J¨ulich High Brilliance Neutron Source (HBS).* Forschungszentrum Jülich GmbH, Zentralbibliothek, Verlag 2020.

9) F. Ott, A. Menelle, and C. Alba-Simionesco, “The sonate project, a french cans for materials sciences research,” in *EPJ Web of Conferences*, vol. 231. EDP Sciences, 2020, p. 0100.

10) L.M Wroe, A.Latina, J. Olivares Herrador et. al. “Accelerator design choices for a Compact Electron-Driven, pulsed neutron source”, in JACoW **LINAC2024** (2024).

Thanks for your attention

Contact: Javier.olivares.herrador@cern.ch

BACK UP SLIDES

III. Unmoderated neutron spectrum

- For the optimized W target, we note:
  - Isotropy in incidence direction θ_i
  - Isotropy in polar detecting angle: Up to 40 deg.
  - Maxwellian neutron emission with $\langle E_n \rangle \sim 1$ MeV
  - **Increase of σ_{E_n}** due to high E_n neutrons; **little change in $\langle E_n \rangle$**

$\langle E_e \rangle$ [MeV]	Y_n [10^{-1} n/e]	f_θ [10^{-2} n/e/sr]	max E_n [MeV]	$f_{E_{n,\mathrm{peak}}}$ [10^{-2} n/e/sr/MeV]
20	0.0407 ± 0.0021	0.045 ± 0.005	0.6	0.047 ± 0.017
50	0.31 ± 0.05	0.350 ± 0.014	0.5	0.33 ± 0.4
100	0.79 ± 0.09	0.879 ± 0.023	0.3	0.77 ± 0.7
300	2.723 ± 0.014	2.89 ± 0.04	0.4	2.42 ± 0.12
500	4.644 ± 0.015	4.77 ± 0.05	0.4	3.89 ± 0.15

Energy neutron spectrum details detected at θ_d = 130 deg

I. Power-Diffusion PDE

- Gradient reduction in terms of figures of merit:

$$-\frac{\partial G_{\text{eff}}}{\partial t} = v_g \frac{\partial G_{\text{eff}}}{\partial z} + \left(-\frac{v_g Q}{r_{\text{eff}}} \frac{\partial (r_{\text{eff}}/Q)}{\partial z} + \frac{\omega}{Q} + \frac{\partial v_g}{\partial z} \right) \frac{G_{\text{eff}}}{2} + \underbrace{\frac{\omega r_{\text{eff}} \tilde{I}}{2Q}}_{\text{Beam Loading term!}}$$

$$-\frac{\partial G_{\text{eff}}}{\partial t} = +\frac{\omega}{Q} \frac{G_{\text{eff}}}{2} - \frac{P_{\text{input}}}{L} + \frac{\omega r_{\text{eff}} \tilde{I}}{2Q}$$

Common features:

- **Beam Loading term**: Decelerating gradient dependent on Intensity.
- **Quasi-static** approximation:
  - Admitted temporal dependency of phasors → G depends on t

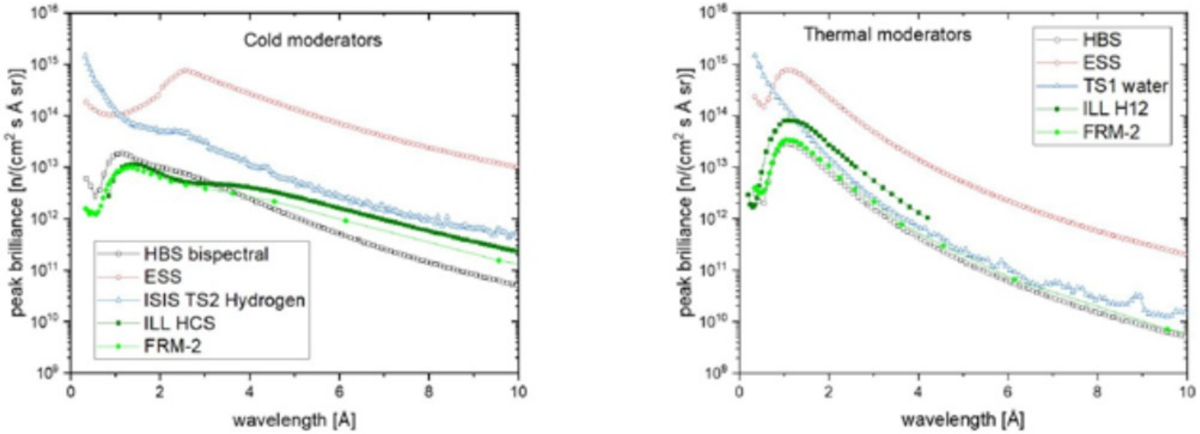

Figure A.4: *Comparison of neutron brilliance of cold (Left) and thermal (Right) neutron yield at various neutron sources*

T. Brückel, T. Gutberlet, J. Baggemann, S. Böhm, P. Doege, J. Fenske, M. Feygenson, A. Glavic, O. Holderer, S. Jaksch et al., *Conceptual Design Report-J¨ulich High Brilliance Neutron Source (HBS).* Forschungszentrum Jülich GmbH, Zentralbibliothek, Verlag 2020.